

# Theory for the nonadiabatic multichannel fragmentation of the $\text{Na}_3^+$ cluster ion following collision with a He atom

D. Babikov and E. A. Gislason<sup>a)</sup>

*Department of Chemistry, University of Illinois at Chicago, Chicago, Illinois 60607-7061*

M. Sizun, F. Aguilon, and V. Sidis

*Laboratoire des Collisions Atomiques et Moléculaires, Unité Mixte de Recherche CNRS-UPS 8625, Bât. 351, Université Paris-Sud, 91405 Orsay Cedex, France*

(Received 15 November 1999; accepted 2 February 2000)

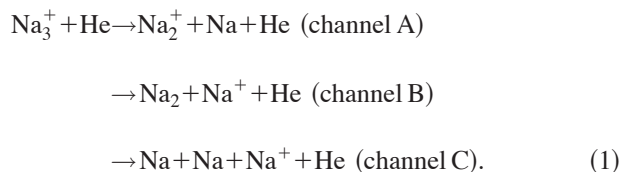
A general theoretical procedure is developed that treats the fragmentation of a polyatomic cluster ion following excitation by a fast rare gas atom. The process involves multiple electronic states of the cluster ion that are described by the diatomics-in-molecule (DIM) procedure. The interaction of the cluster ion with the rare gas atom is obtained by extending the DIM model and by including three-center interactions. The atom-cluster collision is treated using the semiclassical path procedure and the sudden approximation for the cluster. Finally, the fragmentation is studied using the trajectory surface hopping procedure. The method is applied to the  $\text{Na}_3^+$ -He system, which can fragment into three product channels. For each channel doubly differential cross sections are computed and compared with the available experimental data. The calculations give much insight into the fragmentation process of  $\text{Na}_3^+$ . © 2000 American Institute of Physics.

[S0021-9606(00)00916-8]

## I. INTRODUCTION

Collisions of ionic clusters with rare gases at high collision energies have been studied experimentally for many years.<sup>1-7</sup> Typically, the atom excites the cluster in a fast collision, and then the cluster fragments long after the atom has departed. The time separation between the excitation and fragmentation greatly simplifies the analysis. Two general mechanisms have been proposed to explain fragmentation processes, particularly for diatomic clusters.<sup>1,2,6-9</sup> The first is rovibrational excitation (RVE) of the cluster in its electronic ground state by the rare gas atom; if the transferred vibrational and rotational energy is sufficient the cluster will dissociate. The second is electronic excitation (EE) of the cluster by the atom to a repulsive electronic state followed by rapid dissociation to two or more fragments. For a diatomic cluster such as  $\text{H}_2^+$  or  $\text{Na}_2^+$  dissociation along a particular electronic potential curve will usually be adiabatic, because there are typically no avoided crossings with states of the same symmetry. However, for larger clusters avoided crossings between two potential energy surfaces (PESs) are more common, and fragmentation needs not be electronically adiabatic. Transitions between electronic states can mix the RVE and EE mechanisms, and they make any theoretical treatment of the process more challenging.<sup>10,11</sup>

Recently, a systematic experimental study of the fragmentation of sodium clusters,  $\text{Na}_n^+$  ( $2 \leq n \leq 9$ ), in collision with He has been carried out in the collision energy range near 100 eV (center of mass).<sup>3-5</sup> Of particular interest in this paper are the results on the  $\text{Na}_3^+$ +He system, where the following fragmentation processes can occur:



We shall see for this system that there is an avoided crossing in the product region between the ground and first excited PESs that go asymptotically to channels A and B. In addition there is a conical intersection between the first and second excited states when  $\text{Na}_3^+$  has an equilateral configuration.

In this paper we present a general procedure to treat processes such as (1). The method is broken up into four parts. First, the PESs for  $\text{Na}_3^+$  are determined using the diatomics-in-molecules (DIM) procedure.<sup>12,13</sup> The interaction between  $\text{Na}_3^+$  and He is obtained from the DIM model by adding He-Na and He-Na<sup>+</sup> interaction terms, and, in addition, three-center interaction terms involving He are included. Second, the initial conditions of the  $\text{Na}_3^+$  are determined. This is not a trivial matter, because the reactant  $\text{Na}_3^+$  cluster ion can have considerable vibrational energy, and the vibrational motion is not harmonic. The third step treats semiclassically the collision of the  $\text{Na}_3^+$  cluster ion with He.<sup>14</sup> Because the cluster-atom encounter is so fast ( $t_{\text{coll}} \sim 10^{-15}$  s) compared to the cluster vibrations ( $t_{\text{vib}} \sim 10^{-13}$  s), we use the “frozen cluster” approximation to treat this collision. Thus, the Na nuclei are treated as stationary while the He passes by. The  $\text{Na}_3^+$ -He collision produces  $\text{Na}_3^+$  clusters in each of the three electronic states, and it also transfers additional momenta to the three Na nuclei. The final stage of calculation treats the  $\text{Na}_3^+$  fragmentation in the absence of He using the trajectory surface hopping (TSH) method.<sup>15,16</sup> This allows us to properly treat localized nonadiabatic transitions

<sup>a)</sup> Author to whom correspondence should be addressed. Electronic mail: gislason@uic.edu

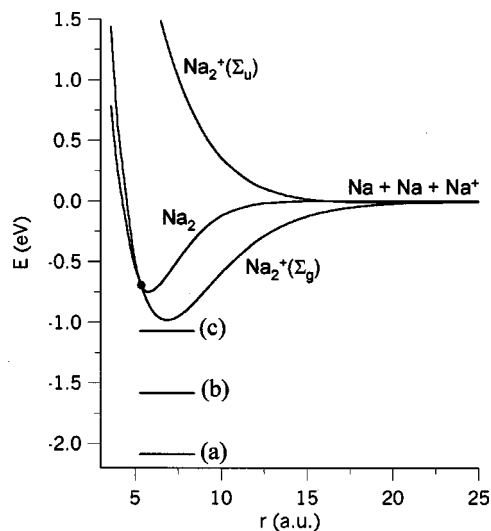


FIG. 1. A cut of the three  $\text{Na}_3^+$  PESs. Shown are the three diatomic curves in the product region with the third Na nucleus at infinity. (These curves are also input to the DIM model.) The crossing between the two lowest curves is shown as a solid circle. The short horizontal lines show the three initial energies of the  $\text{Na}_3^+$  cluster ion studied in this work. The corresponding values of  $E_{\text{int}}$  are (a) 0.02 eV, the zero point energy of  $\text{Na}_3^+$ ; (b) 0.5 eV; (c) 1.0 eV.

between two PESs. A major advantage of this four step procedure is that each step is easily extended to larger systems, such as  $\text{Na}_5^+ + \text{He}$ .

In this paper the theoretical treatment is developed in detail. Then the  $\text{Na}_3^+$  PESs and the interaction with He are presented. Next, total cross sections for the various fragmentation pathways are given as well as doubly-differential cross sections that show the correlation between the center of mass scattering angle and the relative kinetic energy of the cluster fragments. Calculations are carried out for three initial internal energies of the  $\text{Na}_3^+$  cluster ion. The theoretical differential cross sections are compared with the available experimental results.

## II. THEORY

### A. Potential energy surfaces

The PESs and couplings required to investigate the non-adiabatic dynamics of the  $\text{Na}_3^+ - \text{He}$  system in the above-discussed framework have been obtained using the DIMZO method<sup>12</sup> extended by three-center Na-He-Na potential terms. The DIM formalism lends itself to a facile determination of the adiabatic PESs of the cluster and offers the opportunity to easily incorporate the interaction of the helium atom with the cluster. For the  $\text{Na}_3^+$  cluster-ion we follow the treatment of Kuntz,<sup>13</sup> namely, a DIM basis composed of certain low-lying  $\Sigma$  states of the diatomic fragments is chosen. Only singlet states of  $\text{Na}_3^+$  are considered. The three lowest energy diatomic curves used as input are shown in Fig. 1. Certain properties of these curves are summarized in Table I. These curves also represent a cut of the  $\text{Na}_3^+$  PESs in the product region with the third Na nucleus at infinity. The zero of energy corresponds to  $\text{Na} + \text{Na} + \text{Na}^+$ . We see that the ground state dissociates adiabatically to  $\text{Na}_2^+ + \text{Na}$  (channel

TABLE I. Bond lengths and energies for the  $\text{Na}_3^+$  system.<sup>a</sup>

	$r$ (a.u.)	$E$ (eV)
Equilibrium point of $\text{Na}_2^+$	6.86	-0.98
Equilibrium point of $\text{Na}_2$	5.76	-0.75
Equilibrium point of $\text{Na}_3^+$	6.78	-2.12
Conical intersection point <sup>b</sup>	6.78	1.00
Avoided crossing point <sup>c</sup>	5.40	-0.71

<sup>a</sup>The zero of energy corresponds to  $\text{Na} + \text{Na} + \text{Na}^+$ .

<sup>b</sup>Energy of the conical intersection when all three Na-Na distances equal 6.78 a.u.

<sup>c</sup>See Fig. 1.

A), and the first excited state to  $\text{Na}_2 + \text{Na}^+$  (channel B). By comparison, the second excited state is purely repulsive and dissociates to three particles (channel C).

The complete DIM matrix for  $\text{Na}_3^+$  is  $9 \times 9$ . In the valence bond model used here one sodium atom at most can be excited; i.e., the two following configurations are possible,  $\text{Na}(3s) - \text{Na}(3s) - \text{Na}^+$  and  $\text{Na}(3s) - \text{Na}(3p) - \text{Na}^+$ , but the configuration  $\text{Na}(3p) - \text{Na}(3p) - \text{Na}^+$  is not allowed. The adiabatic states of the cluster-ion are obtained as eigenvalues of the Hamiltonian matrix  $\mathbf{H}_0$  in the DIM basis. We call  $\mathbf{C}_0$  the corresponding unitary transformation for  $\mathbf{H}_0$  from the DIM basis to the adiabatic basis; thus,  $\mathbf{C}_0^{-1} \mathbf{H}_0 \mathbf{C}_0$  is a diagonal matrix. The nonadiabatic couplings between the  $\text{Na}_3^+$  adiabatic states, needed in the postcollisional stage of the dynamics, are determined as described in Ref. 17.

A consistent development of the DIM Hamiltonian for the  $\text{Na}_3^+ - \text{He}$  system ( $\mathbf{H} = \mathbf{H}_0 + \mathbf{U}$ ) requires all  $\Sigma$  adiabatic potential curves of the  $\text{He} - \text{Na}^+$ ,  $\text{He} - \text{Na}(3s)$  and  $\text{He} - \text{Na}(3p)$  diatomics to build the  $\mathbf{U}$  matrix. These are calculated using the GAMESS (Ref. 18) code and employ the same basis set and  $l$ -dependent effective-core potential for Na as in Ref. 9. We have also used this program and basis set to calculate a few *ab initio* points for  $\text{Na}_3^+$ . The various diatomic curves are in good agreement with earlier calculations.<sup>19,20</sup>

This procedure was first applied to the  $\text{Na}_2^+ - \text{He}$  system for which an *ab initio* calculation<sup>9</sup> was also available and could be used as a reference. This calculation showed that electronic transitions in the  $\text{Na}_2^+$  dimer are most favored when the helium atom passes between the two Na nuclei. However, the DIM approach of Ref. 13 does not reproduce this important feature. This led us to incorporate in the formalism *three-center-interaction terms* related to interactions of the type  $\langle a | V_{\text{He}} | b \rangle$ , where  $|a\rangle$  and  $|b\rangle$  are  $\text{Na}_A$  and  $\text{Na}_B$   $3s$  and/or  $3p$ -orbitals, and  $V_{\text{He}}$  is the interaction of an electron with a He atom. These short-range three-center-interaction terms have also been included in the  $\text{Na}_3^+ - \text{He}$  system. (The alternative would be to greatly extend the DIM basis set to properly describe the charge delocalization in these metallic clusters.) The interaction was expressed in analytical form as

$$U_{3C} = \alpha R_{\text{He-Na}_A}^n \times \exp\{-\lambda R_{\text{He-Na}_A}\} R_{\text{He-Na}_B}^n \exp\{-\lambda R_{\text{He-Na}_B}\}, \quad (2)$$

TABLE II. Fitting parameters for three-center-interaction terms.<sup>a</sup>

Interaction	Fitting parameters		
	$\alpha$ (a.u.)	$n$	$\lambda$ (a.u.)
Na(3 <i>s</i> )–He–Na(3 <i>s</i> )	0.8622	2.356	1.260
Na(3 <i>s</i> )–He–Na(3 <i>p</i> )	0.0494	2.655	0.5249

<sup>a</sup>The parameters are defined in Eq. (2).

which assumes a nonlocal separable potential for He.<sup>21</sup> The values of the parameters  $\alpha$ ,  $\lambda$ , and  $n$  are given in Table II. They were chosen to best reproduce the two *ab initio* states of Na<sub>2</sub><sup>+</sup>–He when He is located between the two Na nuclei.<sup>9</sup> The DIM interaction between the cluster-ion in its different electronic states and the helium atom is described by the nondiagonal potential energy matrix  $\mathbf{C}_0^{-1}\mathbf{HC}_0$ . The Na<sub>3</sub><sup>+</sup>–He states obtained from this procedure are diabatic<sup>22</sup> with respect to motion of the He atom relative to the cluster, and transitions between electronic states of the cluster arise from off-diagonal matrix elements of the matrix.

The size of the DIM matrices for the Na<sub>3</sub><sup>+</sup> and Na<sub>3</sub><sup>+</sup>–He systems is 9×9.<sup>13</sup> Only the three lowest eigenstates of these matrices, which correlate with channels A, B, and C and dissociate to Na(3*s*) + Na(3*s*) + Na<sup>+</sup>(+He), have been retained in the dynamics. We identify the ground adiabatic state as state 1, and the first and second excited states as states 2 and 3, respectively.

## B. Dynamics

As stated in the Introduction, the dynamics of process (1) is treated in three stages: (1) preparation of the initial conditions of Na<sub>3</sub><sup>+</sup> for the collision; (2) the atom-cluster collision, and, (3) the postcollisional fragmentation of the cluster. A mixture of classical and quantum mechanical methods is used.

### 1. Definition of initial cluster conditions

The semiclassical study of the dynamics of the Na<sub>3</sub><sup>+</sup>–He collision and the subsequent fragmentation require us to define classical initial conditions for the system. In the experimental work,<sup>1–5</sup> the Na<sub>3</sub><sup>+</sup> clusters are probably produced as the result of thermal fragmentation of larger clusters,<sup>23</sup> which were previously ionized by an electron beam. After such a process Na<sub>3</sub><sup>+</sup> clusters in the ground electronic state have negligibly low (thermal) rotational energy, but significant amounts of vibrational excitation (typically up to the dissociation limit of Na<sub>3</sub><sup>+</sup>).

To prepare the initial conditions for such a Na<sub>3</sub><sup>+</sup> cluster ion and to simulate the corresponding distribution of possible cluster shapes we have applied the following statistical algorithm. We start from the equilibrium equilateral geometry of the Na<sub>3</sub><sup>+</sup> cluster. First, 2D-vectors of momenta for each sodium atom are chosen randomly in the cluster plane. Then they are corrected to provide zero angular momentum of the entire cluster. Finally, the momenta of the cluster atoms are scaled by a common factor to provide the needed value of vibrational energy of the cluster. Then the classical Hamilton equations for the motion of the cluster atoms are propagated for a time equal to 100 000 a.u. (~10 vibration periods) plus

$\tau \cdot 30\,000$  a.u., where  $\tau$  is a random number between 0 and 1 and different for each trajectory. The orientation of the cluster plane in space and the relative impact parameter of the He atom are also chosen randomly. The final positions and momenta of each atom are taken as the classical initial conditions for the collisional part of problem.

## 2. Cluster-atom collision

As discussed earlier the He–Na<sub>3</sub><sup>+</sup> collision is fast and is treated by freezing the Na nuclei (the sudden approximation). The results of the collision with He are (i) excitation of the electronic states of Na<sub>3</sub><sup>+</sup>; and (ii) transfer of momentum to each Na nucleus. Because the collision energy is high and because the He atom suffers in most cases only a small deflection (less than 30°), the classical path approximation, a mixed classical-quantum procedure, should work very well.<sup>24</sup> In this case the He atom is assumed to evolve along a classical trajectory  $\mathbf{R}(t)$ , and the time dependent Schrödinger equation is solved along the path for the electronic degrees of freedom of the Na<sub>3</sub><sup>+</sup>. The diabatic picture is used for Na<sub>3</sub><sup>+</sup>–He, and the Schrödinger equation can be reduced to the following system of coupled equations:

$$i\dot{a}_i(t) = \sum_k H_{ik}(\mathbf{R}(t); \mathbf{r}) a_k(t), \quad (3)$$

where  $a_i(t)$  is the probability amplitude for electronic state  $i$  of Na<sub>3</sub><sup>+</sup> ( $i=1,2,3$ ),  $H_{ik}$  is a matrix element of the electronic Hamiltonian  $\mathbf{C}_0^{-1}\mathbf{HC}_0$  (see Sec. II A), and  $\mathbf{r}=(\mathbf{r}_1, \mathbf{r}_2, \mathbf{r}_3)$  is compressed notation for the three fixed vectors that locate the sodium nuclei of the Na<sub>3</sub><sup>+</sup> cluster.

The cluster ion begins in the ground electronic state, but during the collision with He the excited states of Na<sub>3</sub><sup>+</sup> gain population. At these high energies it is well known that the “best” single trajectory  $\mathbf{R}(t)$  follows the path determined by the average potential,

$$\tilde{V}(t; \mathbf{r}) \equiv \sum_{i,k} a_i^*(t) H_{ik}(\mathbf{R}(t); \mathbf{r}) a_k(t). \quad (4)$$

This is the semiclassical energy conserving trajectory method.<sup>14</sup> Similarly, accumulation of momenta by the sodium atoms of the cluster during the collision is calculated by propagation of the following classical equation,

$$\dot{\mathbf{p}} = -\nabla \tilde{V}(t; \mathbf{r}), \quad (5)$$

where  $\mathbf{p}=(\mathbf{p}_1, \mathbf{p}_2, \mathbf{p}_3)$  is compressed notation for the three momentum vectors of the sodium nuclei. The scattering angle of He, which is needed for the comparison with experimental results, can be obtained from  $\mathbf{R}(t_{\text{final}})$ . In addition, the final momenta of the cluster atoms  $\mathbf{p}(t_{\text{final}})$  and the final populations of electronic states

$$c_i = |a_i(t_{\text{final}})|^2 \quad (6)$$

are calculated. They serve as the initial conditions for the postcollisional dynamics of the Na<sub>3</sub><sup>+</sup> cluster.

## 3. Postcollisional cluster dynamics

In contrast to the cluster-atom collision, the postcollisional motion of the cluster is very sensitive to the specific

PES that the trajectory moves on. Electronic transitions can take place at this stage due to nonadiabatic dynamical couplings induced by nuclear motion. These transitions are most probable when the trajectory  $\mathbf{r}(t)$  passes through a region of avoided crossing of two adiabatic PESs (see Fig. 1). The postcollisional fragmentation of  $\text{Na}_3^+$  is investigated using the semiclassical TSH method in the form developed by Parlant and Gislason.<sup>15,16</sup> (Others methods for performing TSH calculations have been developed and successfully applied to a variety of systems.<sup>25,26</sup>) In this procedure the nuclei move classically along one of the three adiabatic PESs, obtained from  $\mathbf{C}_0^{-1}\mathbf{H}_0\mathbf{C}_0$ . The probability amplitudes  $a_i(t)$  for each electronic state are calculated along the trajectory and the dynamical nonadiabatic couplings  $\Omega_{ik}$  between each pair of states are monitored. If a trajectory on surface  $i$  approaches an avoided crossing with surface  $k$  the coupling magnitude  $|\Omega_{ik}|$  will go through a maximum and at that point the trajectory is allowed to branch into two parts. The probability of the surface hop is obtained by integrating the coupled equations for  $a_i(t)$  along the trajectory on the original surface until  $|\Omega_{ik}|$  reaches a minimum at the time  $t_f$ . The probability for the branch on surface  $k$  is then given by  $|a_k(t_f)|^2$ , and the probability for the branch remaining on surface  $i$  is  $1 - |a_k(t_f)|^2$ . On surface  $k$  the Na momenta are adjusted to conserve energy and angular momentum, and the electronic amplitudes on both surfaces are reinitialized. Then both branches of the trajectory are independently propagated forward in time (this is the “ant” version of TSH). Either or both branches can encounter further avoided crossings and the procedure is repeated. The final probability of each branch is equal to the product of various transition and survival probabilities computed at each crossing encountered by that branch. Further details, including the exact procedure for computing the hopping probabilities  $|a_k(t_f)|^2$  and coupling  $\Omega_{ik}$  are given in earlier papers.<sup>15,16</sup>

We start the TSH procedure independently for each electronic state  $i$  that was significantly populated during the  $\text{Na}_3^+$ -He collision. Thus, the final probability of each branch is multiplied by the population  $c_i$  [see Eq.(6)] of state  $i$  after the collision with the He atom. The analysis of the trajectories provides the probability to find the system in a given electronic state with particular positions and momenta of the nuclei. From these data one can decide whether process A, B, or C [see Eq.(1)] has occurred, and obtain various differential cross sections.

### C. Further considerations

The  $\text{Na}_3^+$ -He collision at a center-of-mass kinetic energy  $E_{\text{CM}} = 263$  eV (the energy chosen in the experiments)<sup>4,5</sup> was studied by sampling 50 000 collisions with random selection of initial conditions. The maximum impact parameter of the He atom relative to the center of mass of the cluster was 8 a.u. It is common for a collision with He to transfer insufficient momentum to  $\text{Na}_3^+$  in its ground electronic state so that no fragmentation occurs. These collisions were not considered further. Energy considerations show, however, that electronic excitation to either state 2 or 3 always leads to fragmentation of  $\text{Na}_3^+$ . We observed fragmentation in

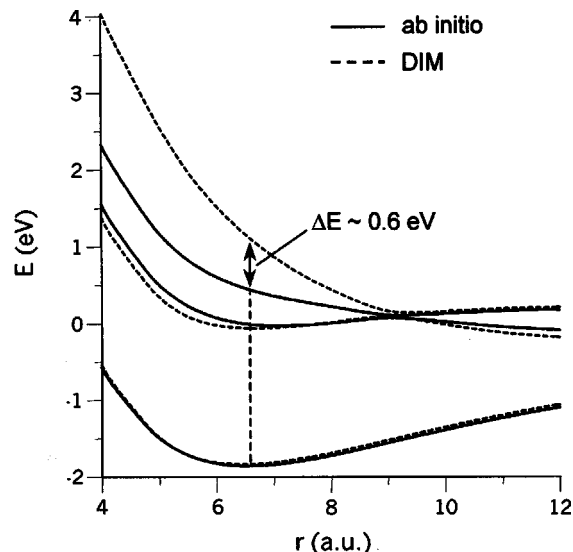


FIG. 2. Comparison of the three DIM  $\text{Na}_3^+$  PESs with *ab initio* values for a T-shaped cluster with  $R$  fixed at 8.0 a.u. The conical intersection of the two excited states is seen at  $r \sim 9.2$  a.u.

approximately 25% of the collisions. Any branch whose probability was smaller than  $5 \cdot 10^{-3}$  was omitted (their overall effect on any cross section was less than one percent). The results of calculations for three values of the initial vibrational excitation of the cluster, 0.02, 0.5, and 1 eV are presented. The first corresponds to the zero-point-energy of the cluster,<sup>27</sup> and the last is just 0.14 eV below the dissociation limit to channel A (see Table I). These values of the vibrational excitation are shown in Fig. 1.

Any process induced by the  $\text{Na}_3^+$ -He collision can be assigned to a particular pathway by specifying the final product channel (A, B, or C) and the electronic state of  $\text{Na}_3^+$  (1, 2, or 3) just after the collision with He. Thus, collision and dissociation into two and three fragments, respectively, on the ground state correspond to pathways A1 and C1. Similarly, excitation of state 2 or 3 by He, followed by adiabatic fragmentation corresponds to pathways B2, C2, or C3. Finally, the “off-diagonal” elements (A2, A3, B1, and B3) correspond to pathways with nonadiabatic transitions during the fragmentation process. Use of the fragmentation matrix implies that there is at most one hop between surfaces during the fragmentation process. (Pathway A3, however, requires a minimum of two hops.) In fact, multiple hops do occur but are rare.

## III. RESULTS AND DISCUSSION

### A. Potential energy surfaces and couplings

In what follows potential energy surfaces (PESs) and couplings will be shown for  $\text{Na}_3^+$  in a T-shaped configuration. Here two Na atoms (the “dimer”) are located on the  $y$ -axis at  $y = r/2$  and  $-r/2$ , and the third atom is located on the  $x$ -axis at  $x = R$ , a distance  $R$  from the center of mass of the dimer. Figure 2 shows a comparison of the DIM surfaces with an *ab initio* calculation at the CI level for the three lowest PESs of  $\text{Na}_3^+$ . In Fig. 2  $r$  is varied and  $R$  is fixed at 8 a.u. The bond lengths shown are typical values where exci-

tation of states 2 and 3 is likely in the  $\text{Na}_3^+ - \text{He}$  collision. The conical intersection between states 2 and 3 is seen when  $r \sim 9.2$  a.u. Kuntz<sup>13</sup> parameterized the DIM model to fit the *ab initio* values of the ground surface. This explains the good fit shown for state 1, and the DIM model is seen to work very well for state 2 as well. At small values of  $r$ , however, the DIM surface for state 3 lies considerably above the *ab initio* surface. This suggests that our calculations of the electronic excitation cross sections for the  $\text{Na}_3^+ - \text{He}$  collision will underestimate the value for state 3, since electronic excitation is strongly dependent on the energy gap. In addition, our calculations will overestimate the kinetic energy release in the complete fragmentation. In all other regards, however, the DIM surfaces are very accurate. In the rest of the paper only DIM surfaces are referred to.

The electronic behavior of  $\text{Na}_3^+$  resembles that of the well-known triangular  $\text{H}_3^+$  ion. There are three low-lying molecular orbitals (MOs) and two valence electrons. The lowest energy MO has no nodes, whereas the two excited MOs each have a single node, one that lies in the  $xz$ -plane perpendicular to  $r$ , and one in a plane perpendicular to the  $x$ -axis that cuts the axis between 0 and  $R$ . The ground state of  $\text{Na}_3^+$ , state 1, has both valence electrons in the ground MO, whereas states 2 and 3 each have one electron in the ground MO and one in an excited MO. When  $\text{Na}_3^+$  has an equilateral shape, the two excited MOs are degenerate and states 2 and 3 are degenerate. We now restrict the discussion to  $r$  fixed at 6.78 a.u., the equilibrium distance of  $\text{Na}_3^+$ . The degeneracy of the equilateral shape can be broken by increasing or decreasing  $R$ . If  $R \sim 20$  a.u., the situation reduces to that shown in Fig. 1.

If  $R$  is reduced but kept to the right of the conical intersection, the wave functions of all three atoms overlap, but the qualitative features remain. State 3 has a minimum in electron density midway between the two nuclei on the  $y$ -axis due to the node in the MO, whereas state 2 has a minimum near  $x = R/2$ . If we plot the interaction between the various states of  $\text{Na}_3^+$  and He, the electron density minima show up as minima in the repulsive potential between  $\text{Na}_3^+$  and He. An example of these potentials for the three states is shown in Fig. 3(a), where  $R = 7.3$  a.u. and  $r = 6.78$  a.u. It is useful in what follows to refer to the three states shown in Fig. 3(a) as diabatic states 1, 2, and 3. Thus, the potential minimum appears along the  $x$ -axis for diabatic state 2 and along the  $y$ -axis for diabatic state 3. Figure 3(b) shows the three interaction potentials for  $\text{Na}_3^+ - \text{He}$  when  $R = 5.3$  a.u., so that the system is to the left of the conical intersection. We see that the qualitative features that describe diabatic states 1, 2, and 3 remain, but now diabatic state 3 is lower in energy than diabatic state 2. This is not surprising, because conical intersections are precisely locations where two diabatic (and two adiabatic) states cross.

Figure 4 shows the PESs when  $r$  is fixed at 6.78 a.u. and  $R$  is varied. The conical intersection between the two upper states in the equilateral cluster shape can be seen. Two arrows show excitation near the conical intersection. One is just to the left of the  $\text{Na}_3^+$  minimum and shows excitation to state 3, and the other is just to the right and shows excitation to state 2. It is also seen that as  $R$  increases, the energy of

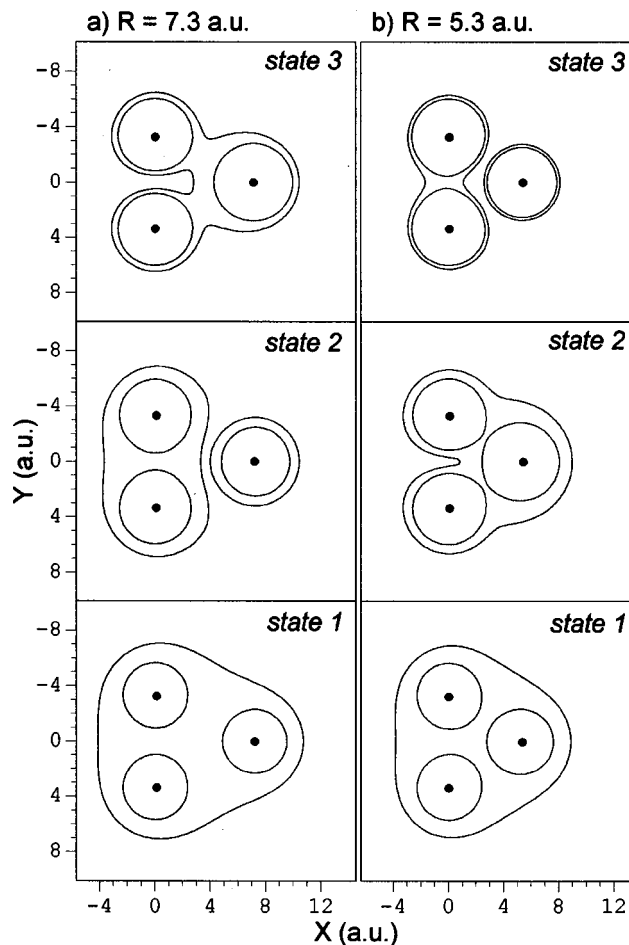


FIG. 3. Interaction potentials between  $\text{Na}_3^+$  and He for the three electronic states. The  $\text{Na}_3^+$  is fixed with coordinates  $(r, R)$  and He moves in the plane of the  $\text{Na}_3^+$ . The energy of one contour was chosen to show the repulsive region around each nuclei, and the other energy was chosen to show the shape of the surface and indicate the role of the node in the excited molecular orbital. (a)  $R = 7.3$  a.u.,  $r = 6.78$  a.u. This is to the right of the conical intersection. The states are (top to bottom) adiabatic state 3 (diabatic state 3), state 2 (diabatic 2), and state 1 (diabatic 1). (b)  $R = 5.3$  a.u.,  $r = 6.78$  a.u. This is to the left of the conical intersection. The states (top to bottom) are adiabatic state 3 (diabatic state 2), state 2 (diabatic 3), and state 1 (diabatic 1).

state 2 falls rapidly and the ground state energy rises. Also shown are the classical turning points for the Na atom when the  $\text{Na}_3^+$  ion has 0.5 and 1.0 eV vibrational energy. At those points the gaps between states 1 and 2 are much smaller, so we expect electronic excitation to have larger cross sections. By comparison, the potential surface for state 3 is relatively flat and vibrational excitation of the  $\text{Na}_3^+$  should not increase the excitation probability. Three-dimensional views of the surfaces have been presented elsewhere.<sup>10</sup>

Of particular interest are the electronic couplings  $H_{12}$  and  $H_{13}$  between the ground state and the two excited states of  $\text{Na}_3^+ - \text{He}$ . (These are the off-diagonal elements in the  $\mathbf{C}_0^{-1} \mathbf{H} \mathbf{C}_0$  matrix.) These couplings are always large when the He is very near one Na nucleus, but collisions with a very small atom-atom impact parameter are rare. In addition, they lead to large deflection angles, so they are not observed in the doubly differential cross sections presented later. Electronic excitation in the processes described here is most im-

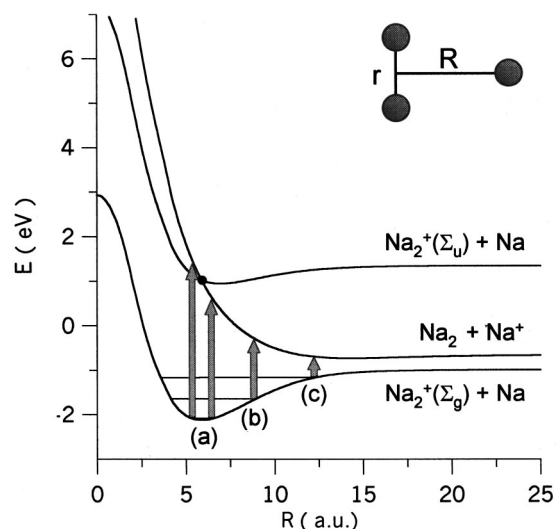


FIG. 4. A cut of the three  $\text{Na}_3^+$  PESs for a T-shaped cluster with  $r$  fixed at 6.78 a.u. (the equilibrium distance of  $\text{Na}_3^+$ ). The conical intersection of the two excited states can be seen at  $R = 5.87$  a.u. The two gray arrows (a) to the left show vertical excitation from near the equilateral potential minimum of  $\text{Na}_3^+$  to state 3 (left arrow) and state 2 (right arrow). The other two show vertical excitations from the outer turning points for  $R$  when  $\text{Na}_3^+$  has 0.5 eV (b) and 1.0 eV (c) vibrational energy.

portant when  $H_{12}$  or  $H_{13}$  is large far from any Na nucleus. Each electronic coupling involves a transition of one electron from the ground MO to the appropriate excited MO, and both are very sensitive to the location of the excited MO nodal surfaces. Inspection of Fig. 3 suggests that the transition between diabatic states 1 and 2 should be very favorable if the He passes between the two Na nuclei on the  $y$ -axis. A similar comparison suggests that the matrix element between diabatic states 1 and 3 should be small in all configurations due to the node in the  $xz$ -plane. This is indeed the case. We have calculated the reduced coupling matrix element  $|H_{13}/(H_{33}-H_{11})|$ , and it is everywhere small except very near the two Na nuclei on the  $y$ -axis. Recalling that diabatic state 3 becomes adiabatic state 2 to the left of the conical intersection, we conclude that the coupling between adiabatic states 1 and 3 is negligible to the right of the conical intersection as is the coupling between adiabatic states 1 and 2 to the left of the intersection.

The diabatic electronic coupling  $H_{12}$  between the ground state and diabatic state 2 is larger and sensitive to the shape of the  $\text{Na}_3^+$  cluster. The reduced coupling  $|H_{12}/(H_{22}-H_{11})|$  when the cluster is cold ( $E_{\text{int}} = 0.02$  eV) is small everywhere except when He is near one of the Na nuclei. By comparison, when  $\text{Na}_3^+$  has 1.0 eV internal energy a typical configuration for excitation to state 2 is quite elongated,  $r = 6.3$  a.u. and  $R = 11.5$  a.u. The reduced coupling to state 2 for this configuration (which lies to the right of the conical intersection) is much bigger than in the case of the cold cluster, and it is, in particular, larger than the energy gap when the He is anywhere between the two Na atoms in the shorter dimer. When  $r = 6.4$  a.u., the repulsive potential for He halfway between the two Na nuclei is about 1 eV, so He can easily pass between the two Na nuclei and excite the cluster without undergoing a significant deflection.<sup>9</sup>

## B. Dynamics calculations

We have calculated total cross sections for each pathway for three values of  $E_{\text{int}}$ , and they are summarized in detail elsewhere.<sup>11</sup> Here we note that most fragmentation originates from the ground electronic state. The cross section for producing state 2 is much larger than for state 3. This is easily explained at  $E_{\text{int}} = 0.5$  and 1.0 eV, because at the outer turning point (see Fig. 4) states 1 and 2 are close in energy, whereas state 3 never approaches state 1. However, at  $E_{\text{int}} = 0.02$  eV the difference is surprising and is attributed to the property of the coupling matrix elements discussed earlier. We saw that state 3 is produced only to the left of the conical intersection, and state 2 only to the right. The smaller energy gap for state 2 then explains its predominance over state 3.

### 1. Cold cluster

The experiments<sup>1-5</sup> have determined doubly differential cross sections for fragmentation. The two independent variables are  $\epsilon$ , the sum of the kinetic energies of the two or three fragments in the  $\text{Na}_3^+$  center of mass reference frame, and  $\chi$ , the scattering angle in the  $\text{Na}_3^+$ -He center-of-mass frame. The intensities are plotted as contour maps as a function of these two variables. Figure 5 shows the results for cold  $\text{Na}_3^+$  clusters ( $E_{\text{int}} = 0.02$  eV). Only those pathways with cross sections greater than  $0.10 \text{ \AA}^2$  are shown. We see that fragmentation that originates in the ground electronic state (A1, C1) involves relatively large deflection angles ( $\chi > 12^\circ$ ), which implies a substantial momentum transfer from He to the  $\text{Na}_3^+$  cluster. We also see that there is a strong correlation between  $\chi$  and  $\epsilon$ , where a larger deflection angle leads to increasing relative energy among the fragments. By comparison, fragmentation due to electronic excitation (pathways B2 and C3) takes place primarily at small scattering angles ( $\chi < 10^\circ$ ). This occurs because electronic excitation is favored when the He atom passes between two nuclei of the  $\text{Na}_3^+$  cluster, and the overall deflection of He is usually small. Also, B2 and C3 appear in concentrated ranges of fragment energies, which can be explained by Franck-Condon considerations in the electronic excitation (see below). By comparison, the ground state processes (A1 and C1) cover a wide range of fragment energies, because fragmentation is driven by impulsive excitation of the  $\text{Na}_3^+$  by He.

The experimentalists recognized that much of their data could be understood by considering a simple energy transfer model.<sup>2,4</sup> This is the "binary" model, where the He atom scatters elastically off one Na atom and does not interact with the other two Na nuclei. This model is described more fully in the Appendix. If the model is applied to pathway A1, it is further assumed that the struck Na is ejected from the  $\text{Na}_3^+$  cluster without interacting with the other two sodium nuclei. The curve for this one-step binary model is shown in Fig. 5 for pathway A1. Overall the agreement is quite good. The model assumes that the  $\text{Na}_2^+$  product is formed with negligible internal energy. Any energy put into  $\text{Na}_2^+$  will decrease  $\epsilon$  for a given  $\chi$ , and lower the data points below the model curve. A careful comparison of the results for pathway A1 in Fig. 5 shows that indeed the results do lie somewhat below the curve, consistent with the trajectory calculations

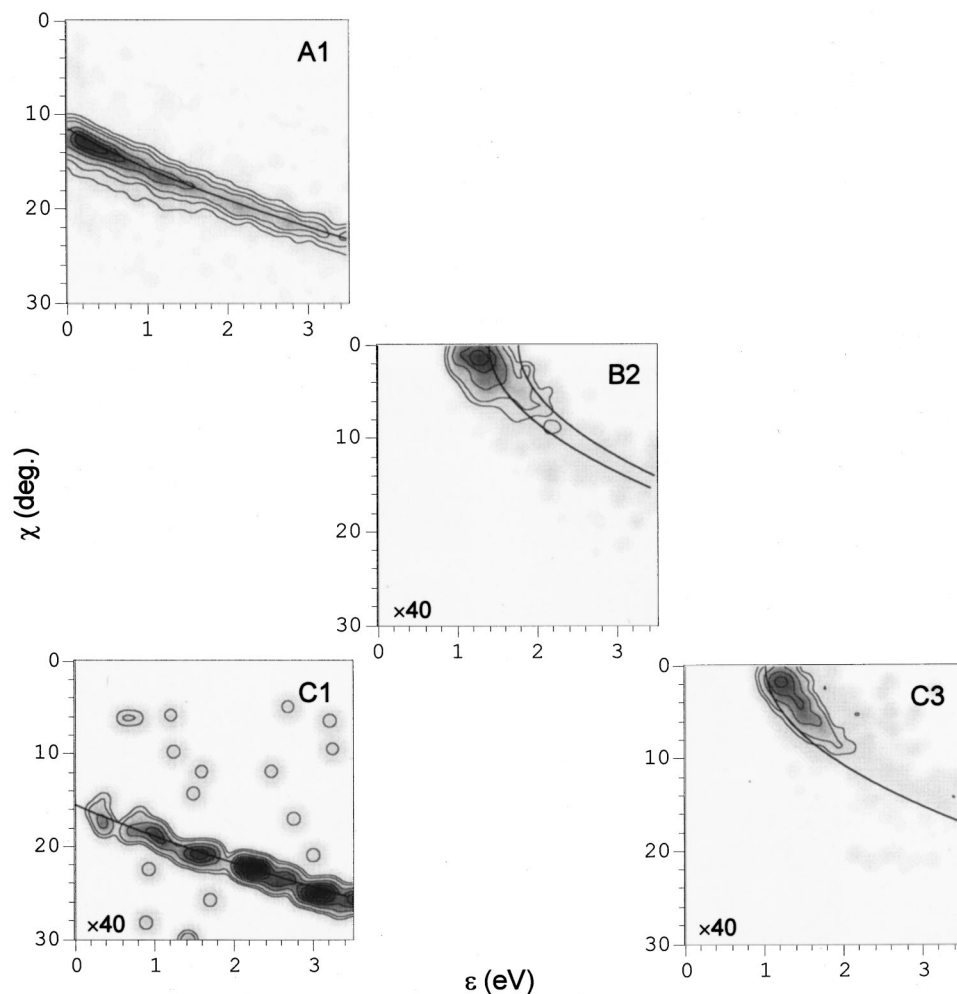


FIG. 5. Intensity contour maps for  $E_{\text{int}}=0.02$  eV plotted as a function of the  $\text{Na}_3^+$ -He COM scattering angle  $\chi$  and the total relative kinetic energy  $\epsilon$  of the fragments. Results are shown for each pathway with a cross section greater than  $0.1 \text{ \AA}^2$ . The various curves are computed for the binary model as described in the text and in the Appendix. For pathway B2 the two curves assume the product  $\text{Na}_2$  has no internal energy (right curve) and 0.37 eV internal energy (left curve).

that show on average the  $\text{Na}_2^+$  dimer is formed with about 0.12 eV internal energy.

The model can be applied to three-body fragmentation (pathway C1). In this case we assume that the struck Na atom shares sufficient energy with the other two Na nuclei to produce three-body dissociation. The binary curve for pathway C1 is shown in Fig. 5. It is clear that the model describes complete fragmentation very well. The small variation of the data above and below the binary curve indicates that the He does interact to some degree with the other two Na atoms. The scattered points far from the curve come from collisions where He hits two Na atoms hard.

The binary model can also be applied to pathways B2 and C3 if additional assumptions are made (see Appendix). We assume that both processes arise from a vertical electronic excitation from the bottom of the  $\text{Na}_3^+$  well to the conical intersection with all three Na-Na bonds equal to 6.78 a.u., and this excitation imparts no deflection to the He atom. At the same time that the electronic excitation is occurring, the He is scattering elastically off one Na atom. This interaction deflects the He by an angle  $\chi$  and adds additional internal energy to the  $\text{Na}_3^+$  cluster as specified by the binary model. Two calculations were done for pathway B2. In one case we assumed that the  $\text{Na}_2$  product has no internal energy ( $E_{\text{dim}}=0$  eV), and in the second we assumed  $E_{\text{dim}}=0.37$  eV, which corresponds to the average internal energy of all prod-

ucts produced in the B2 pathway. Once these various assumptions are made the curves in Fig. 5 are obtained for pathways B2 and C3. Clearly, only qualitative agreement is obtained with the data. For the B2 channel the data lie below both curves. Even more surprisingly the results for C3 shows that the three atoms have more relative energy than the binary model predicts. We attribute both results to the interesting property of the electronic coupling matrix elements discussed earlier. There we saw that the coupling between states 1 and 3 is negligible to the right of the conical intersection, which means that state 3 is produced to the left of the intersection where the potential energy is higher (see Fig. 4). This implies that more energy is released as the  $\text{Na}_3^+$  fragments in pathway C3 than was predicted by the model. In a similar fashion state 2 is produced only to the right of the conical intersection, which means that less energy is available for product recoil for pathway B2. We are not aware of such a dramatic effect due to a conical intersection having been seen before in collision processes. It should be experimentally observable in experiments carried out with cold  $\text{Na}_3^+$  ions.

## 2. Hot cluster

Figure 6 shows the doubly differential cross sections for hot  $\text{Na}_3^+$  clusters ( $E_{\text{int}}=0.5$  eV). The results for 1.0 eV have

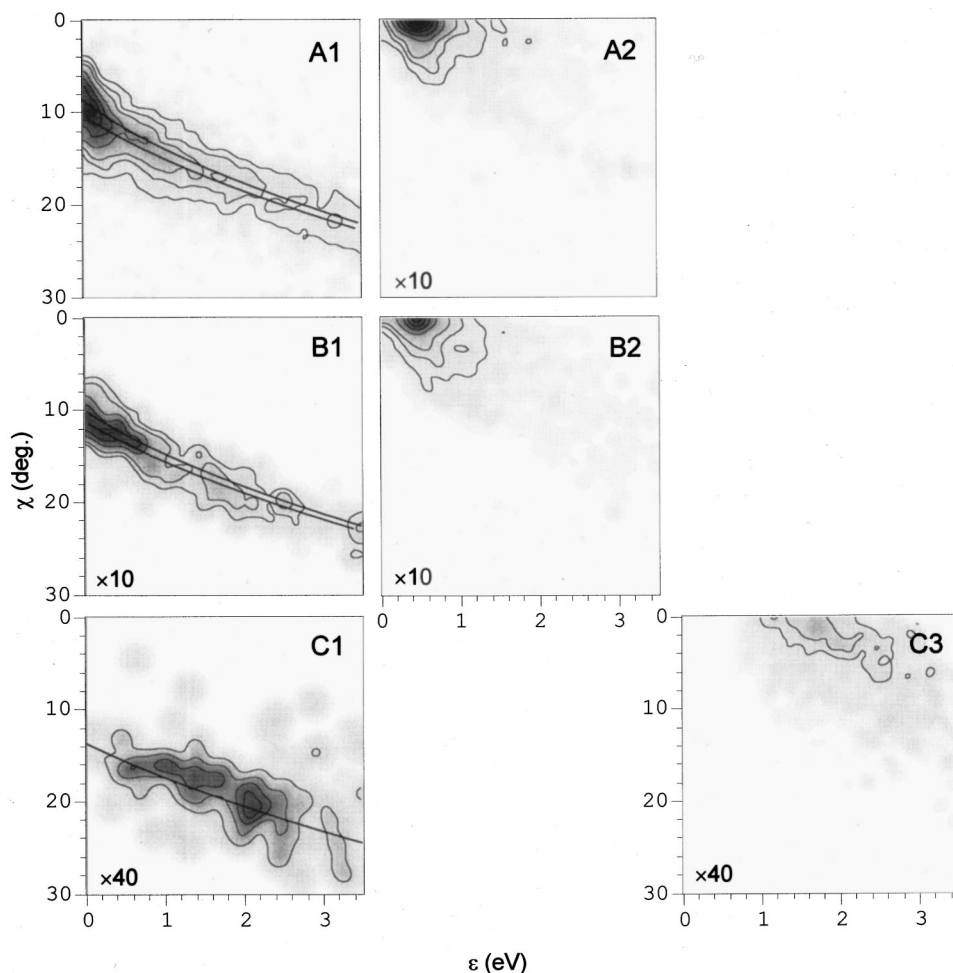


FIG. 6. Intensity contour maps for  $E_{\text{int}}=0.5$  eV. Further details are given in the caption for Fig. 5. For pathway A1 the two curves assume the product  $\text{Na}_2^+$  has no internal energy (upper curve) and 0.27 eV internal energy (lower curve). For pathway B1 the curves assume the  $\text{Na}_2^+$  product has zero (upper curve) and 0.22 eV (lower curve) internal energy.

been presented elsewhere.<sup>10</sup> Now six pathways have appreciable cross sections. As in the previous case we observe a strong correlation between large deflection angles  $\chi$  and large energy release  $\epsilon$ . However, there are a number of significant differences from the results in Fig. 5. For the A1 pathway we now see a feature near  $\chi=6^\circ-10^\circ$  and very small values of  $\epsilon$ . Examination of trajectories shows that this feature is due to fragmentation that results from long-lived  $\text{Na}_3^+$  complexes. In this case the cluster is excited to just above the dissociation limit and only dissociates after a long period of time with minimal kinetic energy release. Our detailed analysis<sup>28</sup> shows that complex trajectories account for about 13% of the A1 pathway when  $E_{\text{int}}=0.5$  eV. They are even more important at  $E_{\text{int}}=1.0$  eV, where 29% of the cross section for pathway A1 comes from the complex mechanism. It is interesting that long-lived complexes are not formed when  $E_{\text{int}}=0.02$  eV (see Fig. 5). The correlation between  $\chi$  and  $\epsilon$  for A1 (as well as for B1 and C1) is similar to what is seen in Fig. 5, but for a given value of  $\epsilon$  the  $\chi$  values are smaller. This reflects the fact that the  $\text{Na}_3^+$  already contains 0.5 eV internal energy, so a softer hit by He is required to cause fragmentation. We also note that the contour maps for A1 and B1 are quite similar. A similar effect is seen for A2 and B2. This indicates that any hop from surface 1 to 2 or vice versa in the fragmentation process has little or no effect on the relative energy of the fragments. We attribute this to

the fact that hops at the crossing seam (see Fig. 1) are induced by vibrational motion of the dimer rather than by translational motion of the fragments.

The location of the  $(\epsilon, \chi)$ -structure for electronic excitation process B2 is different for the cold and hot clusters (compare Figs. 5 and 6). The shift is 0.8 eV for  $E_{\text{int}}=0.5$  eV, and it is even larger (1.0 eV to the left) for  $E_{\text{int}}=1.0$  eV.<sup>10</sup> This can be explained using Franck-Condon considerations (see Fig. 4) and information about the dominant shape of the cold and hot clusters. State 2 is very repulsive in the transition region, and the energy of the fragments decreases considerably when the intermolecular coordinate changes from  $R=6$  a.u. to 8.8 a.u. to 11.5 a.u. By contrast, state 3 is practically flat, so it is not surprising that the energy of the fragments for pathway C3 changes only slightly as  $E_{\text{int}}$  is increased.

The binary model has been applied to the pathways A1, B1, and C1. For the first two cases two curves are shown. The upper curve in both cases assumes that  $E_{\text{dim}}$ , the amount of internal energy in the product dimer, is zero. The lower curve assumes that  $E_{\text{dim}}$  equals the average energy of the dimer products in each pathway (obtained from the trajectory calculations); namely, 0.27 eV for pathway A1 and 0.22 eV for pathway B1. The overall agreement between the data and the model is quite good.

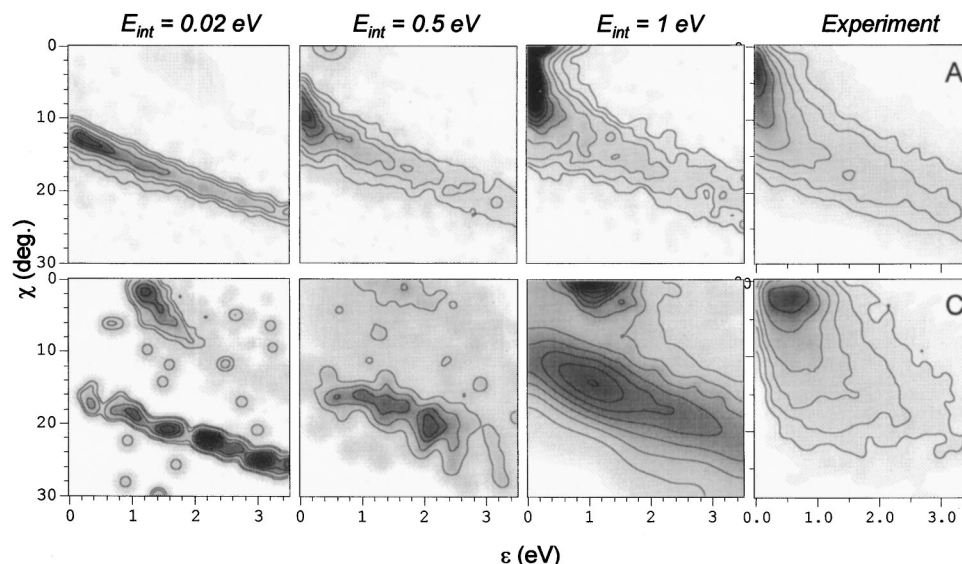


FIG. 7. A comparison of experimental intensity contour maps for fragmentation channels A and C with theoretical results for  $E_{\text{int}}=0.02, 0.5,$  and  $1.0$  eV.  $E_{\text{int}}$  is unknown for the experimental maps. Further details are given in the caption for Fig. 5.

#### IV. COMPARISON WITH EXPERIMENT

Experimental measurements have been made of the doubly differential cross sections for channels A and C. The distribution of internal energies of the  $\text{Na}_3^+$  cluster ions before the collision is not known but is expected to be large. We can compare our theoretical cross sections with the experiments by summing over electronic states 1, 2, and 3. This was done for three values of the internal energy and the comparison is made in Fig. 7. For channel A the experimental results appear to be intermediate between the results for  $E_{\text{int}}=0.5$  and  $1.0$  eV. In particular, it should be noted that the theoretically important contribution of the electronic excitation pathway A2, while not so evident in the experimental results in Fig. 7, was definitely observed in other experimental results<sup>4,5</sup> for channel A.

The results for channel C are also given in Fig. 7. Theory and experiment for the hot clusters show good qualitative agreement, especially for  $E_{\text{int}}=1.0$  eV. In particular, theory provides an explanation of the very broad tail observed experimentally in channel C at large deflection angles. We see that this tail arises from the broad structure of the differential cross section for pathway C1. The tail (FWHM) of the experimental cross section is even wider; presumably this comes from the experimental distribution of internal excitation of the  $\text{Na}_3^+$  ions. The major difference between theory at  $E_{\text{int}}=1.0$  eV and experiment is in the location of the peak structure at small scattering angles due to pathway C3. The theoretical peak value of  $\epsilon$  is  $1.1$  eV, whereas the experimental peak occurs at  $0.5$  eV. This shift of  $0.6$  eV corresponds to the difference in energy between the DIM and *ab initio* surfaces for state 3 in the Franck–Condon region (see Fig. 2). Thus, we believe the difference in the peak locations in Fig. 7 between theory and experimental for channel C is due to the inaccuracies in the DIM surface for state 3.

Overall, the agreement between experiment and theory is best for  $E_{\text{int}}=1.0$  eV. The experimental measurements,<sup>4,5</sup>

limited to the range  $\epsilon < 3.5$  eV,  $\chi < 30^\circ$  of relative fragment energy and scattering angle respectively, yield the values, 90%, 4%, and 6% for the relative populations of channels A, B, and C, respectively. Restricting our results for  $E_{\text{int}}=1.0$  eV to the same window give 79%, 14%, and 7% for channels A, B, and C, respectively. This comparison is judged satisfactory given the lack of information concerning the initial internal energy of the cluster-ion.

#### V. SUMMARY

This paper has presented a general theoretical procedure for studying the fragmentation of polyatomic cluster ions following excitation by a fast rare gas atom. The method allows electronic excitation of the cluster during the atom-cluster collision and also transitions between electronic states at conical intersections and avoided crossings as the cluster fragments. The method can be readily extended to clusters larger than the  $\text{Na}_3^+$  ion studied in this work. The results obtained here demonstrate that the vibrational excitation of the reactant cluster ion will have a dramatic effect on the total and differential cross sections for the various product channels. This occurs both because internal excitation lowers the effective dissociation energy of the cluster ion and because it allows the cluster ion to reach configurations where electronic excitation is more facile. We have also observed extremely interesting results regarding the electronic coupling matrix elements. The presence of a nodal plane in the excited MO makes the coupling between diabatic states 1 and 3 negligible. This then has important consequences for the excitation cross sections and for the kinetic energy release in the products.

The success of the binary model, particularly when  $E_{\text{int}}$  is small, suggests that strong collisions between He and a single Na atom will be one of the major mechanisms for fragmentation of any size  $\text{Na}_n^+$  cluster with any amount of internal excitation. We also believe that the complex mechanism will be important for larger clusters. The various frag-

mentation mechanisms will be examined in more detail in another paper.<sup>28</sup> Finally, our results indicate that the reactant Na<sub>3</sub><sup>+</sup> ions used in the experiments<sup>4,5</sup> are very hot with an average internal energy close to 1.0 eV.

## ACKNOWLEDGMENTS

We would like to thank J. A. Fayeton, M. Barat, and Y. J. Picard at LCAM (Orsay) for providing their experimental data and for helpful discussions.

## APPENDIX: BINARY MODEL

The binary model was developed to describe dimer dissociation<sup>2</sup> and also fragmentation of a cluster with  $n$  atoms.<sup>4</sup> It assumes that the Na <sub>$n$</sub> <sup>+</sup>-He collision involves just one binary He-Na collision and all other Na atoms of the cluster are passive spectators. The transmitted energy does not depend on the particular He-Na potential, and it depends only on the scattering angle of the struck Na atom. For the case of Na<sub>3</sub><sup>+</sup>-He ( $n=3$ ) the following relationship can be obtained:<sup>4</sup>

$$E_{\text{tr}} = \frac{8}{9} \left( \frac{m}{m+M} \right)^2 E_0 \sin^2 \frac{\chi_1}{2}.$$

Here  $E_0$  is the initial cluster energy in the laboratory frame (where He is initially at rest),  $m$  and  $M$  are masses of the He and Na atoms, respectively,  $\chi_1$  is the scattering angle of the struck Na atom in the He-Na center of mass frame, and  $E_{\text{tr}}$  is the transmitted energy in the Na<sub>3</sub><sup>+</sup> center of mass frame. The scattering angle  $\chi$  in the Na<sub>3</sub><sup>+</sup>-He reference frame is related to  $\chi_1$  as follows:

$$\text{tg } \chi = \frac{\sin \chi_1}{\frac{2m}{m+3M} + \cos \chi_1}.$$

These two formulas define the  $E_{\text{tr}}(\chi)$  dependence.

Applying this model to the fragmentation of Na<sub>3</sub><sup>+</sup>, one must account for the initial internal energy of the cluster  $E_{\text{int}}$  and for the final internal energy of the diatomic fragment  $E_{\text{dim}}$  ( $E_{\text{dim}}=0$  for three-body fragmentation). When the model is applied to pathways that involve electronic excitation (such as B2 and C3), the electronic excitation energy  $E_{\text{el}}$  must also be included. In general, the relative energy of the fragments can be calculated as

$$\varepsilon(\chi) = E_{\text{int}} + E_{\text{tr}}(\chi) + E_{\text{el}} - D - E_{\text{dim}},$$

where  $D$  is the dissociation energy to the particular channel (see Table I).

- <sup>1</sup>M. Barat, J. C. Brenot, H. Dunet, and J. A. Fayeton, *Z. Phys. D: At., Mol. Clusters* **40**, 323 (1997).
- <sup>2</sup>J. A. Fayeton, M. Barat, J. C. Brenot, H. Dunet, Y. J. Picard, U. Saalman, and R. Schmidt, *Phys. Rev. A* **57**, 1058 (1998).
- <sup>3</sup>M. Barat, J. C. Brenot, H. Dunet, J. A. Fayeton, and Y. J. Picard, *Comments At. Mol. Phys.* **34**, 329 (1999).
- <sup>4</sup>M. Barat, J. C. Brenot, H. Dunet, J. A. Fayeton, and Y. J. Picard, *J. Chem. Phys.* **110**, 10758 (1999).
- <sup>5</sup>M. Barat, J. C. Brenot, H. Dunet, J. A. Fayeton, Y. J. Picard, D. Babikov, and M. Sizun, *Chem. Phys. Lett.* **306**, 233 (1999).
- <sup>6</sup>J. Durup, in *Recent Developments in Mass Spectrometry*, edited by K. Ogata and T. Hayakawa (University of Tokyo Press, Tokyo, 1970), p. 921.
- <sup>7</sup>J. Los and T. R. Govers, in *Collision Spectroscopy*, edited by R. G. Cooks (Plenum, New York, 1978), p. 289.
- <sup>8</sup>M. Sizun and E. A. Gislason, *J. Chem. Phys.* **91**, 4603 (1989).
- <sup>9</sup>D. Babikov, F. Aguillon, M. Sizun, and V. Sidis, *Phys. Rev. A* **59**, 330 (1999).
- <sup>10</sup>D. Babikov, M. Sizun, F. Aguillon, and V. Sidis, *Chem. Phys. Lett.* **306**, 226 (1999).
- <sup>11</sup>D. Babikov, E. A. Gislason, M. Sizun, F. Aguillon, and V. Sidis, *Chem. Phys. Lett.* **316**, 129 (2000).
- <sup>12</sup>P. J. Kuntz, in *Atom-Molecule Collision Theory*, edited by R. B. Bernstein (Plenum, New York, 1979), p. 79.
- <sup>13</sup>P. J. Kuntz, *Mol. Phys.* **88**, 693 (1996).
- <sup>14</sup>A. E. DePristo, *J. Chem. Phys.* **78**, 1237 (1983).
- <sup>15</sup>G. Parlant and E. A. Gislason, *J. Chem. Phys.* **91**, 4416 (1989).
- <sup>16</sup>M. Sizun, J. B. Song, and E. A. Gislason, *J. Chem. Phys.* **109**, 4815 (1998).
- <sup>17</sup>P. J. Kuntz, in *Atom-Molecule Collision Theory*, edited by R. B. Bernstein (Plenum, New York, 1979), p. 105.
- <sup>18</sup>M. Schmidt, K. K. Baldrige, J. A. Boatz, S. T. Elbert, M. S. Gordon, J. H. Jensen, S. Koseki, N. Matsunaga, K. Q. Nguyen, S. J. Su, T. L. Windus, M. Dupuis, and J. A. Montgomery, *J. Comput. Chem.* **14**, 1347 (1993).
- <sup>19</sup>J. Pascale, Technical Report, Service de Physique des Atomes et des Surfaces, 1991, C.E.N. Saclay, Gif-sur-Yvette Cédex, France.
- <sup>20</sup>G. Theodorakopoulos and I. D. Petsalakis, *J. Phys. B* **26**, 4367 (1993).
- <sup>21</sup>V. Sidis, C. Kubach, and D. Fussen, *Phys. Rev. A* **27**, 2431 (1983).
- <sup>22</sup>V. Sidis, in *Advances in Chemical Physics Series, State-Selected and State-to-State Ion-Molecule Reaction Dynamics, Part 2, Theory*, edited by Michael Baer and C. Y. Ng (Wiley, New York, 1992), p. 73.
- <sup>23</sup>L. Bewig, U. Buck, Ch. Mehlmann, and M. Winter, *J. Chem. Phys.* **100**, 2765 (1994).
- <sup>24</sup>E. Gislason, G. Parlant, and M. Sizun, in *Advances in Chemical Physics Series, State-Selected and State-to-State Ion-Molecule Reaction Dynamics, Part 2: Theory*, edited by Michael Baer and C. Y. Ng (Wiley, New York, 1992), p. 321.
- <sup>25</sup>J. C. Tully, *Faraday Discuss.* **110**, 407 (1998).
- <sup>26</sup>M. S. Topaler, T. C. Allison, D. W. Schwenke, and D. G. Truhlar, *J. Chem. Phys.* **110**, 687 (1999).
- <sup>27</sup>F. Wang and E. I. Von Nagy-Felsobuki, *Mol. Phys.* **77**, 1197 (1992).
- <sup>28</sup>D. Babikov, E. A. Gislason, M. Sizun, F. Aguillon, and V. Sidis, *J. Chem. Phys.* (accepted, 2000).